Available online at www.sciencedirect.com

ScienceDirect

Current Opinion in Biomedical Engineering

Emerging imaging modalities for functional assessment of donor lungs *ex vivo*

Maria R. Hudock[1], Meghan R. Pinezich[1], Seyed Mohammad Mir[2], Jiawen Chen[2], Matthew Bacchetta[3,4], Gordana Vunjak-Novakovic[1,5] and Jinho Kim[2]

Abstract

The severe shortage of functional donor lungs that can be offered to recipients has been a major challenge in lung transplantation. Innovative *ex vivo* lung perfusion (EVLP) and tissue engineering methodologies are now being developed to repair damaged donor lungs that are deemed unsuitable for transplantation. To assess the efficacy of donor lung reconditioning methods intended to rehabilitate rejected donor lungs, monitoring of lung function with improved spatiotemporal resolution is needed. Recent developments in live imaging are enabling non-destructive, direct, and longitudinal modalities for assessing local tissue and whole lung functions. In this review, we describe how emerging live imaging modalities can be coupled with lung tissue engineering approaches to promote functional recovery of *ex vivo* donor lungs.

Addresses

[1] Department of Biomedical Engineering, Columbia University, New York, NY, USA
[2] Department of Biomedical Engineering, Stevens Institute of Technology, Hoboken, NJ, USA
[3] Department of Cardiac Surgery, Vanderbilt University, Nashville, TN, USA
[4] Department of Biomedical Engineering, Vanderbilt University, Nashville, TN, USA
[5] Department of Medicine, Columbia University, New York, NY, USA

Corresponding authors: Kim, Jinho (jkim6@stevens.edu); Vunjak-Novakovic, Gordana (gv2131@columbia.edu)

Current Opinion in Biomedical Engineering 2023, **25:**100432

This review comes from a themed issue on **Intelligent Biomaterials in Biomedical En**

Edited by **Melissa Skala**, **Francisco Robles**, and **Irene Georgakoudi**

For complete overview of the section, please refer the article collection - Intelligent Biomaterials in Biomedical En

Received 23 June 2022, revised 14 November 2022, accepted 23 November 2022

https://doi.org/10.1016/j.cobme.2022.100432

Keywords

Lung transplantation, Donor lung reconditioning, Imaging, *Ex vivo* lung Perfusion, Tissue engineering.

Introduction

For patients with end-stage lung disease, lung transplantation is the only definitive therapeutic option [1]. Unfortunately, nearly 80% of donor lungs are disqualified for transplantation, mainly due to poor gas exchange function resulting from lung injury prior to procurement. The availability of transplantable donor lungs could be substantially increased if injured donor lungs, many of which are of marginal quality, can be repaired to a level that meet acceptable transplant criteria [2–4]. Innovative donor lung reconditioning protocols and platforms, such as isolated [5] and cross-circulation [2,6–8] *ex vivo* lung perfusion (EVLP), have been developed with the goal of improving the functional integrity of rejected donor lungs.

A technological bottleneck hampering donor lung reconditioning is that current methods used to evaluate lung function during EVLP treatments provide only limited insight into the progression of lung recovery. Current lung function evaluation methods are largely limited to monitoring global (i.e., not region-specific) parameters associated with lung injury. Notably, imaging modalities that are *i*) capable of mapping local lung function, *ii*) noninvasive/nondestructive, and *iii*) operational in real time would help clarify why individual donor lungs fail or improve during EVLP. The imaging-assisted approach to donor lung reconditioning can aid in planning interventions, administering treatments tailored to individual lung (region) needs, and monitoring responses in a closed-loop manner. By enabling a mechanistic understanding of lung injury, interventions, and recovery, the imaging-based approach can be leveraged to expand the pool of donor lungs acceptable for transplantation (Figure 1).

Here, we discuss selected clinical and research-level imaging technologies reported within the last five years that can be used to quantify specific functions of three distinct anatomical compartments of the lung: *i*) respiratory tract, *ii*) alveolar gas exchange region, and *iii*) vasculature. We focus on functional imaging methods which generate localizable signals and which are applicable to *ex vivo* support platforms for donor lungs.

Donor lung injury modes and critical functions

Donor lungs are susceptible to a variety of complications, which may be global or region-specific (preferentially affecting airways, parenchyma, vasculature, or a subset of any of these). These complications include

Figure 1

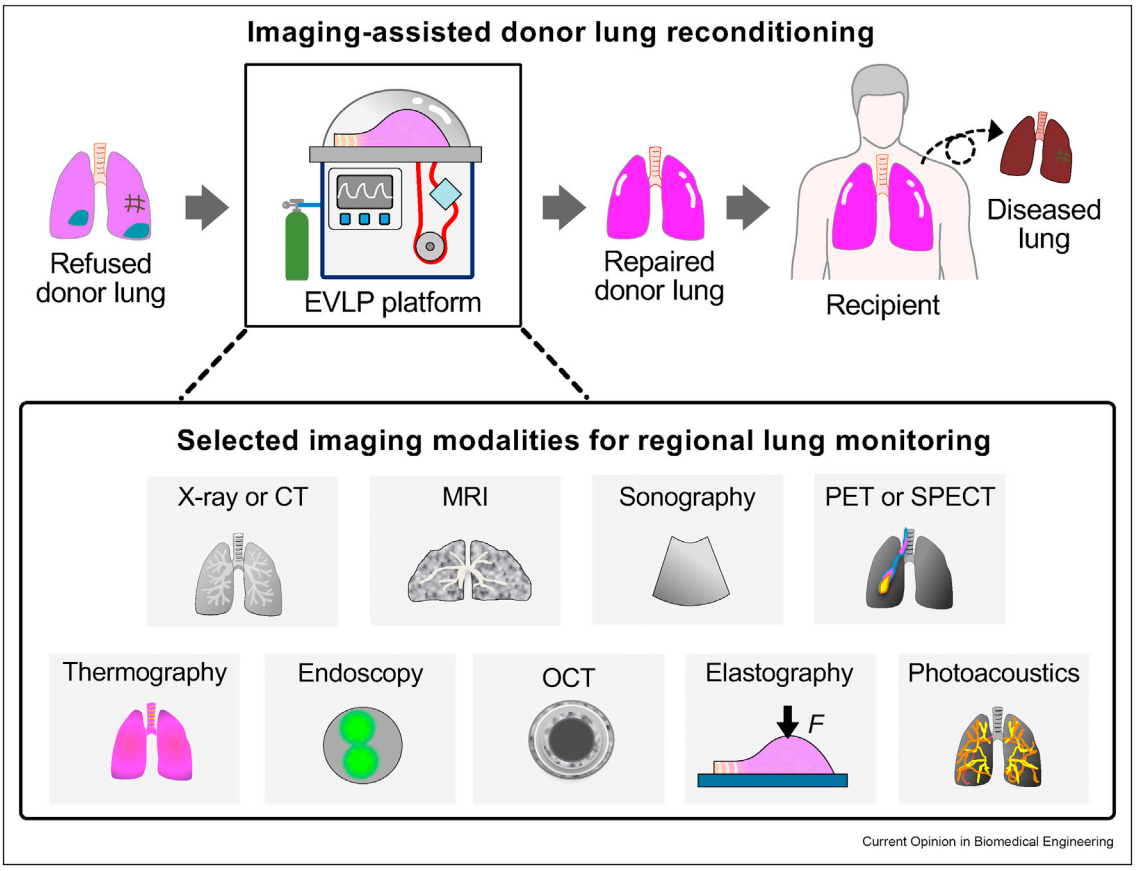

Imaging-assisted donor lung reconditioning. Selected real-time functional imaging modalities for detecting regional lung deficits, assisting in targeted repair, and monitoring lung recovery during rehabilitation of disqualified donor lungs on *ex vivo* support platforms. CT: computed tomography; MRI: four-dimensional MRI; PET: positron emission tomography; SPECT: single-photon emission computed tomography; OCT: optical coherence tomography.

atelectasis, contusion or hemorrhage due to trauma, edema due to leaky vasculature, pulmonary emboli, and perimortem aspiration in the donor [2]. While EVLP aims to recover donor lungs injured by various mechanisms, adjunct technologies that enable real-time, non-destructive functional monitoring of different lung regions may facilitate directed injury repair. Thus, we have identified critical functions to monitor in three distinct lung compartments:

i) Respiratory tract (conducting airways: trachea through terminal bronchioles): Critical functions include mucociliary clearance and ventilation. Mucociliary clearance is the directional removal of inhaled pathogens or particles by an "escalator" of mucus driven by beating cilia. Ventilation refers to the movement of air in and out of the lung.
ii) Lung parenchyma (gas exchange region: respiratory bronchioles through alveoli): Critical functions include gas exchange and elastic deformation. Gas exchange involves oxygen and carbon dioxide equilibration between alveoli and the bloodstream, while elastic recoil is the main driver of exhalation during normal breathing.
iii) Pulmonary vasculature: Critical functions include vessel patency, responsiveness, permeability, and immune recruitment. Patency refers to vessel openness, i.e., not blocked by clots or stenosis. Permeability refers to the status of tight junctions in the endothelium, supporting normal tissue fluid balance. Immune recruitment refers to transport of cellular and humoral contents to the lung via the vasculature in response to infection and injury.

In a donor lung of substandard quality, certain functions may be more compromised than others, depending on the cause and mechanism of injury. In the following sections, we discuss possible applications of cutting-edge imaging technologies to quantify these critical lung functions, which together may set a foundation for advanced lung recovery platforms.

Imaging-assisted monitoring of respiratory tract functions

Mucociliary clearance

Mucociliary clearance is typically measured by tracking the movement of inhaled tracers as they are transported by ciliary action. Several noninvasive methods utilize radiation: gamma scintigraphy of the chest has been used to track the clearance of technetium-based radiolabeled particles in numerous studies [9]. Scintigraphy, however, is limited to averaged mucociliary clearance because it is difficult to determine the exact location of the tracers in the airways (e.g., small vs. large airways) from the 2D images acquired. To access airway-level detail, methods with increased spatial and temporal resolution have been developed. In one approach, tantalum microparticles delivered into the lungs were traced using X-ray computed tomography (CT) (Figure 2a). Not only was the clearance of individual particles in 3D visualized with high temporal resolution, but also a new phenomenon was observed: elastic recoil of cystic fibrosis mucus [10]. Another method that employed positron emission tomography (PET) was able to track bulk movement of distally instilled radiotracers along the entire course of the respiratory tract [11] (Figure 2b).

Radiation-free methods have also been developed, including the use of fluorescent nanoparticles in mucociliary clearance tracking in thin tissues with traditional microscopy [12]. This particle tracking method can also be applied to larger tissues via intratracheal insertion of optical fiber imaging probes in fluorescence micro-bronchoscopy. For example, we created a fluorescence micro-bronchoscopy device that is capable of resolving and tracking single fluorescently labeled microparticles or cells that are coated on the airway lumen of isolated rat lungs. This imaging modality could be extended to human-sized *ex vivo* lungs [6,13,14]. It is possible in particle-based imaging that particles are not fully cleared from the lung. Micro-bronchoscopy could be used to visualize ciliary action in a particle-free manner via cilia-targeted fluorescent labels, such as fluorescent wheat germ agglutinin [15]. Label-free quantitative assessments of airway tissue structure and function can be achieved through optical coherence tomography (OCT). Advanced OCT systems can provide cross-sectional views of airway epithelium with high imaging resolution ($\sim$1–3 μm), enabling direct visualization of cilia movement. Inclusion of tracer particles allows for simultaneous measurement of mucus micro-rheology and mucociliary clearance [16,17]. Given the many existing uses and advanced bronchoscopy for OCT, it is expected that this technique will be easily extended to human-sized lungs [18,19]. Considerations of specialty equipment, radiation exposure, and desired temporal and spatial scales will determine which of these imaging methods are most appropriate for investigating donor lung regeneration.

Ventilation in the conducting zone

Clinical techniques such as X-ray and bronchoscopy assess the general condition of conducting airways in *ex vivo* lungs. These add to the functional data that can be gleaned from mechanical ventilator readings, such as peak inspiratory pressure and lung compliance [8]. However, these methods are limited by poor individual airway resolution (X-ray) or cumbersome sampling of one airway at a time, and to imaging of larger airways (bronchoscopy). The leading clinical systems for evaluating airway dynamics are four-dimensional (4D = 3D + time) computed tomography (4DCT) and magnetic resonance imaging (4DMRI). Both modalities can generate local flow-volume relations (Figure 2c), display regional differences in tissue strain throughout the entire lung, and be used to monitor localized lung injures [20–22]. These measures would be useful for planning local interventions and monitoring regional donor lung recovery. 4DCT is considered the clinical gold standard, but 4DMRI offers the additional advantage of eliminating radiation exposure in the *ex vivo* donor lung [23]. A few other CT-based technologies can provide complementary information. Inferences can be made about global small airway health using conventional CT images and parametric response mapping, which was recently shown to correlate to micro-CT of tissue [24]. For localized detail, phase contrast CT can be used to capture individual terminal bronchiole opening and closure during ventilation [25] (Figure 2d).

Sound-based technologies, stemming from one of the oldest lung monitoring modalities, the stethoscope, are comparatively low-cost and rapidly implementable methods of monitoring airway condition. For example, turbulent flow in large airways and closure/reopening in small airways have distinctive auditory signatures (stridor and crackles, respectively), which can be regionally resolved. Crackles, in particular, may signal abnormal surfactant properties, which in turn inform the functional wellbeing of type II alveolar cells, while stridor signals constriction of larger airways. Sound-based technologies include both auscultation and forced oscillation measurement systems, which, combined with advanced signal processing methods, are capable of discriminating features of multiple pulmonary diseases [26–29]. These technologies have been further reviewed recently [30]. In total, 4DCT may be the most powerful technology for tracking lung recovery, with 4DMRI perhaps soon to follow. Parametric response mapping and acoustic technologies, as a less resource-intensive alternatives, might be more realistic for immediate adoption.

Imaging-assisted monitoring of lung parenchyma

Gas transport and exchange

Spatially heterogeneous tissue defects are a common feature of refused donor lungs, but conventional

methods used to measure gas exchange function of lung provide only averaged readouts across the whole lung. In contrast, MRI can allow region-by-region functional assessments of *ex vivo* donor lungs. Using an inhalable contrast agent, such as xenon-129 gas (^{129}Xe), MRI permits three-dimensional, high-resolution, and longitudinal lung function measurements without using radiation [31–33] (Figure 3a). Inhaled ^{129}Xe can readily dissolve in lung tissue and red blood cells (RBC). Notably, ^{129}Xe resonates at distinct frequencies when

Figure 2

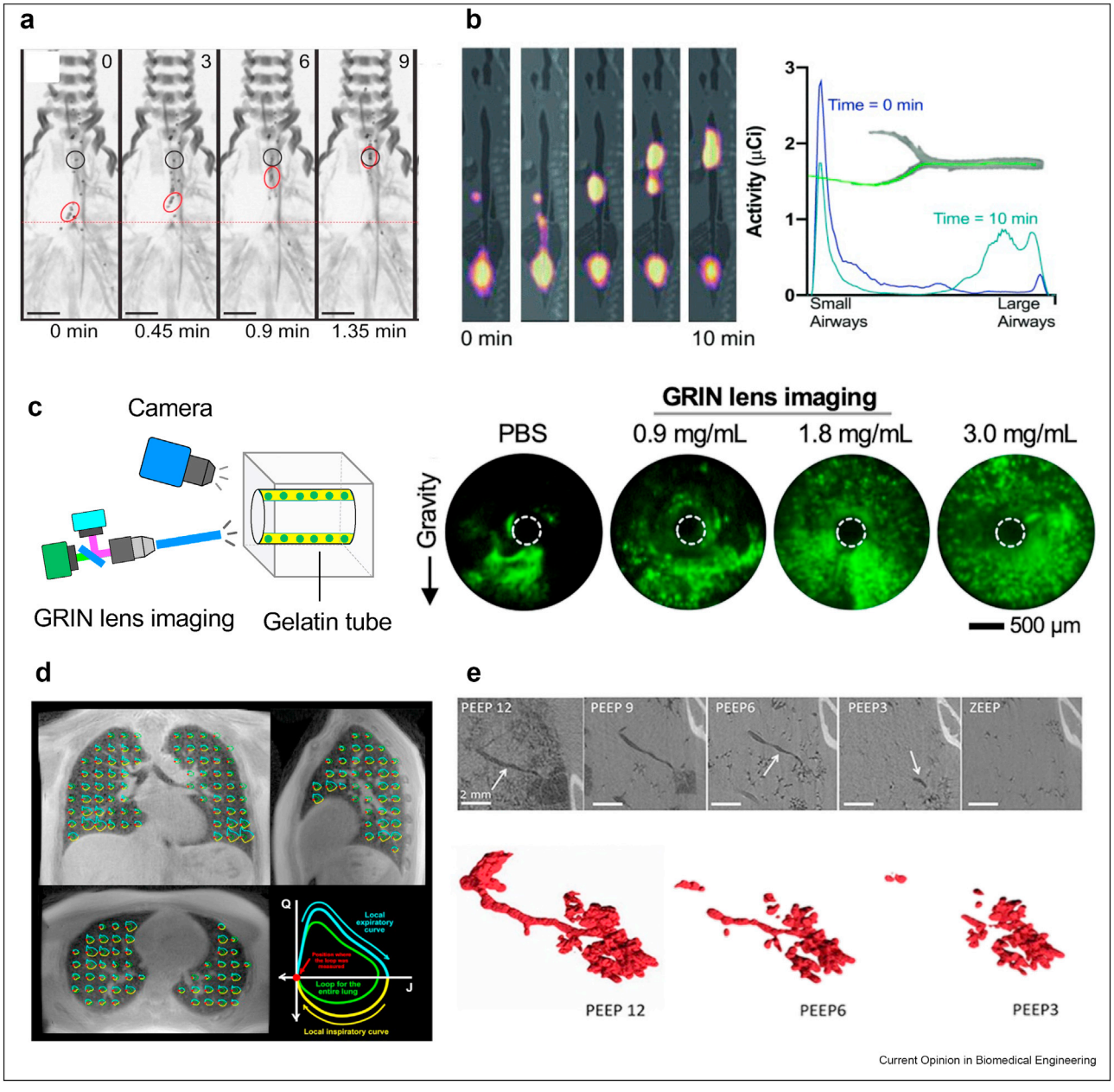

Functional imaging of mucociliary clearance and ventilation in the conducting zone airways. (a) Tantalum microdisk path tracking by CT [10]. (b) PET signal transport by MCC, overlayed on CT image (left) and traced along 3D airway reconstruction (right) [11]. (c) Schematic of bronchoscope-deployable GRIN lens-based fluorescence imaging probe (left) and acquired images of 10 μm fluorescent particles deposited intraluminally via collagen hydrogels of varying concentrations [14]. (D) 4DMRI flow-volume loops plotted for 1/20th of points tracked, with lung-average loops superimposed on each local loop, demonstrating regional variation [21]. (d) Progressive closure of a single terminal bronchial under decreasing PEEP observed with phase-contrast CT [25]. 4DMRI: four-dimensional magnetic resonance imaging; CT: computed tomography; GRIN: gradient-index; MCC: mucociliary clearance; PEEP: positive end-expiratory pressure; PET: positron emission tomography.

dissolved in air, alveolar tissue, and blood, allowing accurate estimation of gas transport between the airspace and vascular network [34]. Importantly, the materials used to construct the platform for *ex vivo* support of lungs imaged by ^{129}Xe MRI must not interact with the magnetic fields. Further, the trade-off between measurement resolution and associated costs will need to be evaluated.

Real-time visualization of oxygen uptake can be achieved at reduced cost via multispectral fluorescence microscopy (Figure 3b) and photoacoustic microscopy (PAM)

Figure 3

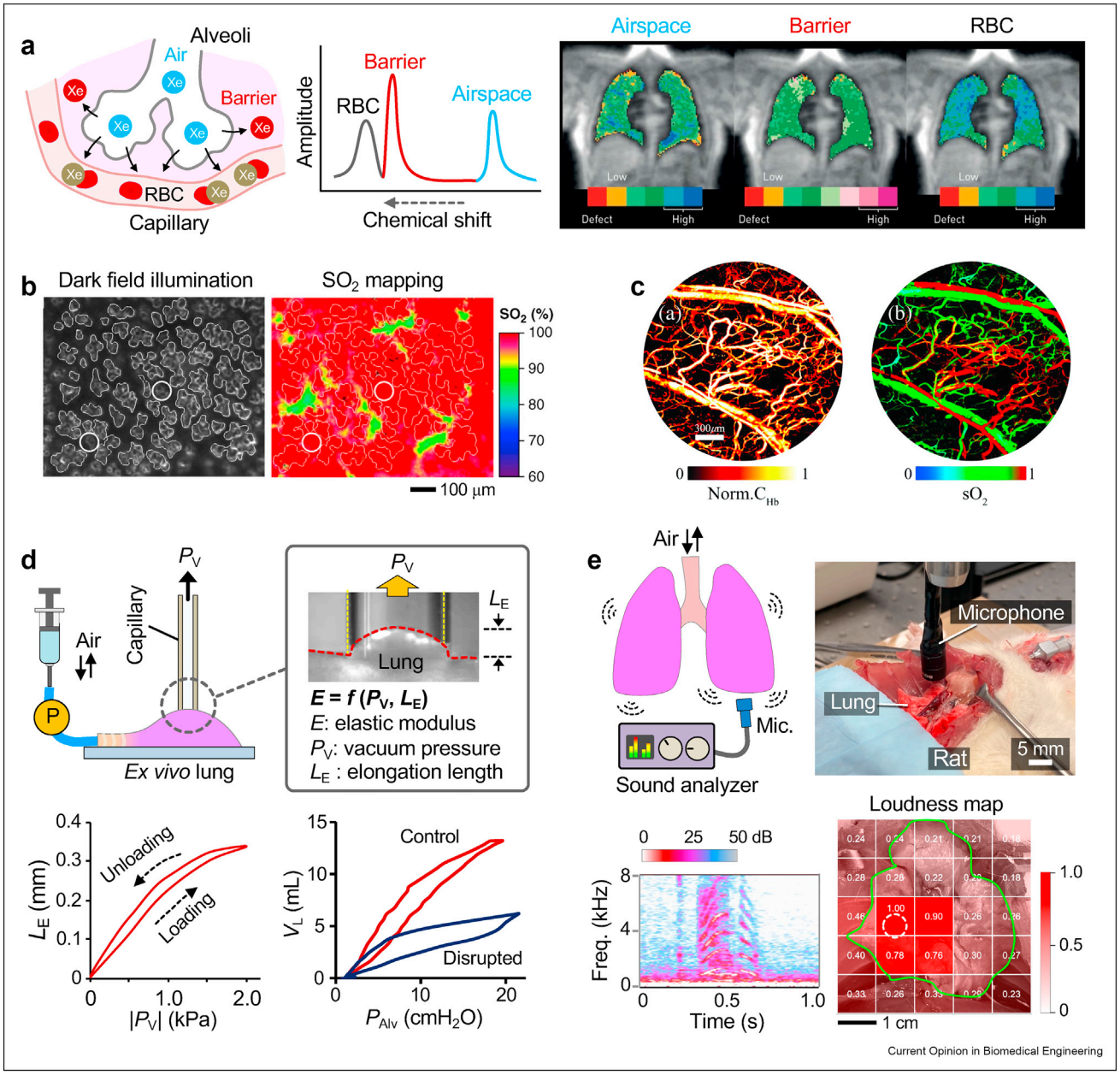

Imaging-assisted structural and functional assessment of lung parenchyma. (a) Real-time noninvasive monitoring of gas transport and exchange of lung via ^{129}Xe MRI [33]. Barrier: alveolar tissue barrier. RBC: red blood cell. (b) 2D visualization of oxygen saturation level (sO_2) across lung tissue via multispectral fluorescence microscopy (MFM) [35]. (c) 3D visualization of hemoglobin concentration (C_{Hb}) and sO_2 within a biological tissue via photoacoustic microscopy (PAM) [37]. (d) Non-destructive region-by-region quantification of lung tissue stiffness via vacuum-enabled tissue tensile test [41] (e) Assessment of structural and functional integrity of lung parenchymal tissue via sound-assisted airflow quantification [29]. Freq: frequency, Mic: microphone.

[35–38] (Figure 3c). The underlying principle of both imaging methods is that hemoglobin (Hb) absorbs light differently when it is oxygenated (HbO_2) and deoxygenated (HbR). Therefore, oxygen saturation (sO_2) and hemoglobin concentration (C_{Hb}) can be determined by quantifying absorption of the excitation lights in tissue. Wavelengths between 650 nm and 900 nm are typically used because they are much more highly absorbed by HbO_2 and HbR than by water, leading to improved signal-to-noise ratios [35,36]. While multispectral fluorescence microscopy can determine sO_2 distributions only at the tissue surface due to considerable light scattering within tissue, photoacoustic methods can generate 3D sO_2 maps with excellent imaging resolution in deeper tissue regions (up to several centimeters). The superior imaging quality and depth of photoacoustic microscopy are due to detection of acoustic waves, which scatter less than light in biological tissues [37,38]. However, because acoustic waves propagate poorly in airspaces, photoacoustic sO_2 quantification may also be limited to subpleural regions.

Elastic tissue deformation

The ability of lung tissue to repeatedly deform (i.e., stretch and contract) in response to applied force or pressure is a useful measure to characterize the quality of *ex vivo* donor lungs [39,40]. Deformability of lung tissue, which varies spatially across a lung, can be determined by directly measuring stiffness (i.e., elasticity) of local tissue. We established a vacuum-based elastography method that enables accurate quantification of tissue stiffness in a localized, real-time, and nondestructive manner [41] (Figure 3d). In this approach, lung parenchymal tissue at a selected region is elongated by locally applying a vacuum pressure. By correlating the length of tissue elongation (L_E) and the magnitude of vacuum pressure applied (P_V), we determined the elastic moduli (E) of lung tissue. Notably, measured L_E varied nonlinearly in response to loading-unloading of P_V and exhibited hysteresis, which is a unique behavior of lung tissue and agrees with observations by 4DCT and 4DMRI. Further, this method allowed measuring the elasticity of acutely injured lung tissue. Of note, lung tissue stiffness at low lung volume is mainly determined by the surface tension of the pulmonary surfactant, while at higher lung volumes, the lung tissue matrix elasticity becomes increasingly important in determining stiffness. This suggests that elastography can allow independent, quantitative assessment of both surfactant properties and matrix elasticity simply by taking measurements at different lung volumes. Using this method, tissue stiffness maps that visually describe multiple aspects of tissue integrity across the *ex vivo* lung can be obtained.

Integrity of lung parenchymal tissue can also be evaluated by measuring acoustic signals (i.e., sounds) emitted from the lung during ventilation [30,42] (Figure 3e). As air travels through the airways of the lung or escapes via damaged tissue, distinct sound signals at specific frequencies are generated due to dynamic interaction between the airflow and surrounding tissues [43]. Thus, lung sounds can be used to quantify ventilation, monitor lung function, or diagnose lung pathologies. In our recent study, we demonstrated that the location and severity of acute lung tissue defects could be determined by analyzing respiratory sound signals [29]. Using the acquired sound data, a 2D acoustic map was generated that accurately predicted the location and severity of tissue damage. Significantly, due to external placement of acoustic sensors (e.g., microphones) for the measurements, acoustic mapping could be used for convenient longitudinal monitoring not just *ex vivo*, but also once lungs are repaired and implanted *in vivo*.

Imaging-assisted monitoring of pulmonary vasculature

Perfusion and patency

Donor lung vascular condition, including patency, perfusion, and vessel responsiveness to vasoconstrictive or vasodilatory factors, has been shown to correlate with transplant outcomes, but methods to evaluate vasculature condition *in situ* remain limited [2,44]. Thus, *ex vivo* vascular evaluation is valuable to the entire transplant process, in addition to its role in recovery interventions on EVLP. Perfusion of the pulmonary vasculature enables oxygen transport, temperature regulation, and clearance of cellular debris. Clinical methods to evaluate perfusion have also been applied to *ex vivo* donor lungs, including radiography, sonography, and scintigraphy [45,46]. These methods for imaging the whole lung can be used to globally assess perfusion throughout all lobes and peripheral regions of the donor lung (Figure 4a). Furthermore, multiparametric oxygen-enhanced MRI can detect regional lung injury and impaired gas exchange prior to lung transplantation, which was demonstrated in a preclinical model of ischemic injury [47] (Figure 4b).

Because the lungs serve as a biological heat exchanger in which heat is transferred from circulating blood to inhaled, ambient-temperature air, the surface temperature of the *ex vivo* lungs can also indicate effective regional perfusion. Accordingly, thermography has been applied to donor lungs as a means of assessing the uniformity and distribution of perfusion, including in swine lungs with ischemic and gastric aspiration injuries and in human donor lungs [2,7,8,44]. Gross thermography of the whole lung enables identification of regions with poor perfusion that may benefit from additional targeted therapies. Further, focal thermography monitors temperature changes following contact application of a cold probe to the surface of the lung, serving as a marker for regional vascular health (Figure 4c). In swine lungs supported on EVLP, thermography has been used to

Figure 4

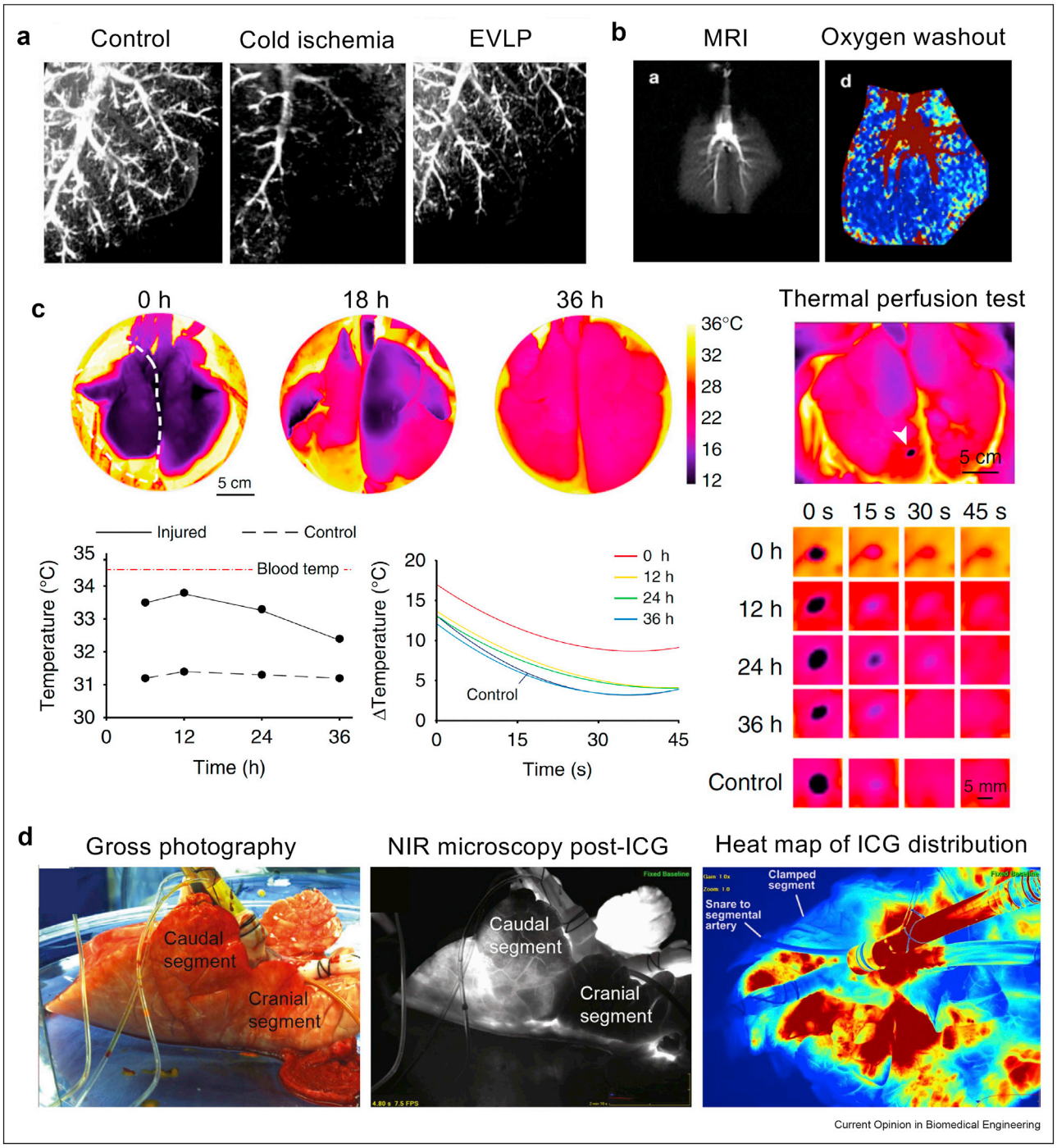

Modalities for functional imaging of pulmonary vasculature. (a) Micro-computed tomography angiography to visualize patency and perfusion of pulmonary vasculature in control, cold ischemic, and *ex vivo* lung perfusion (EVLP) rat lungs [46]. (b) Magnetic resonance imaging (MRI) of pulmonary vasculature with heat map demonstrating oxygen washout [47]. (c) Thermography of swine lung supported with cross-circulation EVLP for real-time monitoring of perfusion, (i) thermographs obtained at 0, 18, 36 h of perfusion, (ii) thermal perfusion test with cold probe application followed by real-time temperature monitoring, (iii) quantification of lung temperature in control, gastric injury, and following cold probe application [2]. (d) Visualization of perfusion using near infrared microscopy (NIR) of indocyanine green (ICG) following intravenous delivery into *ex vivo* swine lung [51].

assess surface temperature prior to transplantation. Early surface temperature (8 min post-reperfusion) was determined to be a reliable indicator of pulmonary function and transplant suitability, with improved transplant outcomes in lungs with surface temperature $\geq$26 °C [48].

Blood vessel permeability

The vascular barrier is essential for maintaining tissue homeostasis. In injured lungs, pulmonary edema occurs frequently due to disrupted vascular permeability, leading to fluid buildup in the interstitium and parenchyma as well as impaired gas exchange. Methods to evaluate edema in donor lungs *ex vivo* typically rely on measurement of donor lung weight gain (i.e., changes in the wet/dry ratio or lung weight), which is imprecise and not standardized. Because compromised vasculature is a main contributor to pulmonary edema, monitoring of vascular permeability in *ex vivo* donor lungs may be useful for assessing donor lung suitability for transplantation. Recently, a clinical study utilized ultrasound of human lungs on EVLP to determine the ability of the "direCt Lung Ultrasound Evaluation (CLUE)" scoring system to predict transplant outcomes [49]. Furthermore, delivery of fluorescent tracers within the pulmonary vasculature followed by real-time imaging enables visualization and assessment of vascular integrity and permeability [50]. For example, near-infrared fluorescence imaging of delivered indocyanine green has been applied for *ex vivo* and *in situ* monitoring of pulmonary edema and vascular integrity [50–52] (Figure 4d). While fluorescent microspheres also have been tested as the tracer, the intense inflammatory response they generate in the host prohibits their usage *in vivo* [53].

Immune recruitment

In addition to structural integrity and patency of the pulmonary vasculature, the composition (e.g., cell populations, inflammatory markers, etc.) recruited to the lung via the vascular compartment may offer further insight into lung health. Recent advances in intravital imaging have demonstrated novel approaches towards functional and compositional evaluation of the vascular compartment, including to quantify the fraction of functional microvasculature in the pulmonary microcirculation; detection of endotoxins present in the blood, which attract immune components; and circulation of exogenous therapeutic cells following delivery [54–56]. These intravital imaging techniques could be extended to use in *ex vivo* donor lungs to assess the impact of injury on inflammatory and immune constituents in the pulmonary vasculature. Overall, imaging modalities for visualization of pulmonary vasculature should allow high-resolution assessment of all lung regions and utilize bioinert and immune-compatible contrast agents. Delivery of therapeutics that simultaneously enable visualization could further serve theranostic (therapeutic + diagnostic) applications in the pulmonary vasculature.

Conclusions and outlook

Real-time, non-destructive imaging enables the study of lung repair and regeneration in greater detail, with attention to functional recovery. The end-goal of incorporating more advanced imaging technology is to increase the number of lung available for transplant by rescuing rejected donor lungs. The technologies discussed here offer a range of resolutions, scales, costs, and utilities. Clinically adjacent technologies, such as advanced CT and MRI, offer the best whole-lung resolution across several lung functions, while their drawbacks include high operation costs and the need for specialty tracers [10,32]. Several methods that can be deployed bronchoscopically, such as fluorescence micro-bronchoscopy and OCT, are suited to highly localized assessments of lung tissue. Thermography, elastography, and auscultation represent accessible methods for measuring integrity of lung parenchyma or vasculature. Notably, prior to procurement, nearly all donor lungs are evaluated for their suitability for transplantation via chest X-ray or CT. Therefore, the lung function data acquired by new and advanced lung imaging modalities can be compared with the radiographically obtained baseline information of the rejected donor lung to quantitatively evaluate the efficacy of EVLP treatments.

With recent rapid advancements in tissue engineering and stem cell technologies, removing damaged lung cells and replacing them with a healthy cell population is one of the key strategies being pursued towards recovering donor lungs with advanced damage. To make this donor lung bioengineering approach feasible, the research community needs improved methods that allow *in situ* cell replacement and longitudinal monitoring of their regenerative activities. Some of the imaging modalities discussed above can be useful to expedite realization of this innovative donor lung reconditioning strategy. For instance, fluorescence micro-bronchoscopy, OCT, and intravital imaging methods may be particularly well suited for guiding cell removal and delivery into selected lung regions and for follow-up imaging with cellular level detail. Meanwhile, 4DCT, 4DMRI, and ^{129}Xe MRI may be suited to quantifying the organ-wide alterations associated with cell removal and implantation, and subsequent lung function improvement. Thus, equipped with these real-time, nondestructive, and region-specific functional imaging modalities, donor lung regeneration strategies may more rapidly advance towards clinical use.

Declaration of competing interest

The authors declare that they have no known competing financial interests or personal relationships that could have appeared to influence the work reported in this paper.

Data availability

Data will be made available on request.

Acknowledgements

The authors acknowledge and the National Institutes of Health (grant P41 EB027062 to GVN), the National Science Foundation (CAREER Award 2143620 to JK), New Jersey Health Foundation (PC 5-21 to JK), and American Thoracic Society Foundation (Unrestricted Research Grant to JK) for funding support.

References

Papers of particular interest, published within the period of review, have been highlighted as:

* of special interest
** of outstanding interest

1. Labaki WW, Han MK: **Chronic respiratory diseases: a global view**. *Lancet Respir Med* Jun. 2020, **8**:531–533. https://doi.org/10.1016/S2213-2600(20)30157-0.

2. Guenthart BA, *et al.*: **Regeneration of severely damaged lungs using an interventional cross-circulation platform**. *Nat Commun* July 2019, **10**:1985. https://doi.org/10.1038/s41467-019-09908-1.

3. Young KA, Dilling DF: **The future of lung transplantation**. *Chest* Mar. 2019, **155**:465–473. https://doi.org/10.1016/j.chest.2018.08.1036.

4. Valapour M, *et al.*: **OPTN/SRTR 2020 annual data report: lung**. *Am J Transplant* 2022, **22**:438–518. https://doi.org/10.1111/ajt.16991.

5. Cypel M, *et al.*: **Normothermic ex vivo lung perfusion in clinical lung transplantation**. *N Engl J Med* Apr. 2011, **364**:1431–1440. https://doi.org/10.1056/NEJMoa1014597.

6. Kim J, Guenthart B, O'Neill JD, Dorrello NV, Bacchetta M, Vunjak-Novakovic G: **Controlled delivery and minimally invasive imaging of stem cells in the lung**. *Sci Rep* Oct. 2017, **7**. https://doi.org/10.1038/s41598-017-13280-9. Art. no. 1.

7. O'Neill JD, *et al.*: **Cross-circulation for extracorporeal support and recovery of the lung**. *Nat. Biomed. Eng.* Mar. 2017, **1**. https://doi.org/10.1038/s41551-017-0037. 0037.

8. ** Hozain AE, *et al.*: **Xenogeneic cross-circulation for extracorporeal recovery of injured human lungs**. *Nat Med* Jul. 2020, **26**. https://doi.org/10.1038/s41591-020-0971-8. Art. no. 7.
Hozain et al. report the use of a xenogeneic cross-circulation platform to recover injured human donor lungs. Throughout 24 h of cross-circulation support, donor lungs demonstrated gross, histomorphologic, radiographic, and functional improvements. Imaging modalities utilized include real-time thermography, angiography, and bronchoscopy to evaluate perfusion and patency of the pulmonary vasculature and structural integrity and inflammation in the airways.

9. Donaldson SH, Corcoran TE, Laube BL, Bennett WD: **Mucociliary clearance as an outcome measure for cystic fibrosis clinical research**. *Proc Am Thorac Soc* Aug. 2007, **4**:399–405. https://doi.org/10.1513/pats.200703-042BR.

10. * Pino-Argumedo MI, *et al.*: **Elastic mucus strands impair mucociliary clearance in cystic fibrosis pigs**. *Proc Natl Acad Sci USA* Mar. 2022, **119**, e2121731119. https://doi.org/10.1073/pnas.2121731119.
Pino-Argumedo et al. report a method of tracking mucociliary clearance that gives insight into local phenomena, not just bulk transport. Tantalum microdisks are insufflated into the lungs and used as a contrast agent visible by X-ray computed tomography as they are carried along with mucus transport. With this method, the authors were able to observe for the first time the elastic recoil of would-be cleared mucus in a cystic fibrosis animal model.

11. Stewart CG, *et al.*: **Measurement of mucociliary transport: novel application of positron emission tomography**. In *2022 IEEE 19th international symposium on biomedical imaging (ISBI)*; Mar. 2022:1–5. https://doi.org/10.1109/ISBI52829.2022.9761605.

12. Rogers TD, Ostrowski LE, Livraghi-Butrico A, Button B, Grubb BR: **Mucociliary clearance in mice measured by tracking trans-tracheal fluorescence of nasally aerosolized beads**. *Sci Rep* Oct. 2018, **8**. https://doi.org/10.1038/s41598-018-33053-2. Art. no. 1.

13. Mir SM, *et al.*: **Imaging-guided bioreactor for de-epithelialization and long-term cultivation of ex vivo rat trachea**. *Lab Chip* Mar. 2022, **22**:1018–1031. https://doi.org/10.1039/D1LC01105G.

14. ** Chen J, *et al.*: **Homogeneous distribution of exogenous cells onto de-epithelialized rat trachea via instillation of cell-loaded hydrogel**. *ACS Biomater Sci Eng* Jan. 2022, **8**:82–88. https://doi.org/10.1021/acsbiomaterials.1c01031.
Chen et al. developed a bioreactor for *ex vivo* support of rat trachea with built-in imaging capabilities. Using fluorescence micro-bronchoscopy to monitor delivered products with cell-level resolution, they demonstrated advanced tissue manipulations such as decellularization and uniform reseeding of cells along the entire interior of a trachea sustained on the reactor up to four days.

15. Nakamura R, *et al.*: **A novel method for live imaging of human airway cilia using wheat germ agglutinin**. *Sci Rep* Sep. 2020, **10**. https://doi.org/10.1038/s41598-020-71049-z. Art. no. 1.

16. Liu L, *et al.*: **Method for quantitative study of airway functional microanatomy using micro-optical coherence tomography**. *PLoS One* Jan. 2013, **8**:e54473. https://doi.org/10.1371/journal.pone.0054473.

17. Chu KK, *et al.*: **Particle-tracking microrheology using micro-optical coherence tomography**. *Biophys J* Sep. 2016, **111**:1053–1063. https://doi.org/10.1016/j.bpj.2016.07.020.

18. Goorsenberg A, Kalverda KA, Annema J, Bonta P: **Advances in optical coherence tomography and confocal laser endomicroscopy in pulmonary diseases**. *Respiration* 2020, **99**:190–205. https://doi.org/10.1159/000503261.

19. Pahlevaninezhad H, *et al.*: **Nano-optic endoscope for high-resolution optical coherence tomography in vivo**. *Nat Photonics* Sep. 2018, **12**:540–547. https://doi.org/10.1038/s41566-018-0224-2.

20. Xiong G, Chen C, Chen J, Xie Y, Xing L: **Tracking the motion trajectories of junction structures in 4D CT images of the lung**. *Phys Med Biol* Jul. 2012, **57**:4905–4930. https://doi.org/10.1088/0031-9155/57/15/4905.

21. Boucneau T, Fernandez B, Larson P, Darrasse L, Maître X: **3D magnetic resonance spirometry**. *Sci Rep* Jun. 2020, **10**. https://doi.org/10.1038/s41598-020-66202-7. Art. no. 1.

22. ** Herrmann J, *et al.*: **Quantifying regional lung deformation using four-dimensional computed tomography: a comparison of conventional and oscillatory ventilation**. *Front Physiol* 2020, **11**. Accessed: May 31, 2022. [Online]. Available: https://www.frontiersin.org/article/10.3389/fphys.2020.00014.
Herrmann et al. applied four-dimensional computed tomography (4DCT) to compare magnitude and regional variation in tissue strain under different ventilation protocols. Using the localized strain information obtained from 4DCT, they found that multi-frequency oscillatory ventilation resulted in lower strain across all regions than during other ventilation protocols, which is important for avoiding ventilator-induced lung injury.

23. Zhang J, *et al.*: **Clinical evaluation of 4D MRI in the delineation of gross and internal tumor volumes in comparison with 4DCT**. *J Appl Clin Med Phys* 2019, **20**:51–60. https://doi.org/10.1002/acm2.12699.

24. Vasilescu DM, *et al.*: **Noninvasive imaging biomarker identifies small airway damage in severe chronic obstructive pulmonary disease**. *Am J Respir Crit Care Med* Sep. 2019, **200**:575–581. https://doi.org/10.1164/rccm.201811-2083OC.

25. Broche L, *et al.*: **Individual airway closure characterized in vivo by phase-contrast CT imaging in injured rabbit lung**. *Crit Care Med* Sep. 2019, **47**:e774. https://doi.org/10.1097/CCM.0000000000003838.

26. Rodgers GW, Lau Young JB, Desaive T, Shaw GM, Chase JG: **A proof of concept study of acoustic sensing of lung recruitment during mechanical ventilation**. *Biomed Signal Process Control* Feb. 2017, **32**:130–142. https://doi.org/10.1016/j.bspc.2016.08.021.

27. Ngo C, *et al.*: **Assessing regional lung mechanics by combining electrical impedance tomography and forced oscillation technique**. *Biomed. Eng. Biomed. Tech.* Dec. 2018, **63**:673–681. https://doi.org/10.1515/bmt-2016-0196.

28. Begin G, AL-Tamimi KM, Alamdari HH, Witter T, El-Sankary K: **Lung mechanics tracking with forced oscillation technique (FOT) based on CMOS synchronous demodulation principle**. *IEEE Trans. Biomed. Circuits Syst.* 2022:1–13. https://doi.org/10.1109/TBCAS.2022.3186161.

29. ** M. R. Pinezich *et al.*, "Sound-guided assessment and localization of pulmonary air leak," Bioeng. Transl. Med., vol. n/a, no. n/a, p. e10322, doi: 10.1002/btm2.10322.This paper describes a sound-based method for assessment of lung parenchyma integrity. This study is the first study to demonstrate severity and location of lung tissue injury that causes pulmonary air leak can be identified by analyzing the acoustic signals directly collected across the injured lung.

30. Rao A, Huynh E, Royston TJ, Kornblith A, Roy S: **Acoustic methods for pulmonary diagnosis**. *IEEE Rev. Biomed. Eng.* 2019, **12**:221–239. https://doi.org/10.1109/RBME.2018.2874353.

31. Driehuys B, Cofer GP, Pollaro J, Mackel JB, Hedlund LW, Johnson GA: **Imaging alveolar–capillary gas transfer using hyperpolarized 129Xe MRI**. *Proc Natl Acad Sci USA* Nov. 2006, **103**:18278–18283. https://doi.org/10.1073/pnas.0608458103.

32. Möller HE, *et al.*: **MRI of the lungs using hyperpolarized noble gases**. *Magn Reson Med* 2002, **47**:1029–1051. https://doi.org/10.1002/mrm.10173.

33. Wang Z, *et al.*: **Diverse cardiopulmonary diseases are associated with distinct xenon magnetic resonance imaging signatures**. *Eur Respir J* Dec. 2019, **54**. https://doi.org/10.1183/13993003.00831-2019.

34. Niedbalski PJ, *et al.*: **Protocols for multi-site trials using hyperpolarized 129Xe MRI for imaging of ventilation, alveolar-airspace size, and gas exchange: a position paper from the 129Xe MRI clinical trials consortium**. *Magn Reson Med* 2021, **86**:2966–2986. https://doi.org/10.1002/mrm.28985.

35. Tabuchi A, *et al.*: **Acute lung injury causes asynchronous alveolar ventilation that can Be corrected by individual sighs**. *Am J Respir Crit Care Med* Feb. 2016, **193**:396–406. https://doi.org/10.1164/rccm.201505-0901OC.

36. Ayala L, *et al.*: **Band selection for oxygenation estimation with multispectral/hyperspectral imaging**. *Biomed Opt Express* Mar. 2022, **13**(3):1224–1242. https://doi.org/10.1364/BOE.441214.

37. * Liu C, Chen J, Zhang Y, Zhu J, Wang L: **Five-wavelength optical-resolution photoacoustic microscopy of blood and lymphatic vessels**. *Adv. Photonics* Jan. 2021, **3**. https://doi.org/10.1117/1.AP.3.1.016002. 016002.
This paper reports optical-resolution photoacoustic microscopy (OR-PAM) integrated with five different pulsed excitation lights. This imaging method is capable of *in vivo* measurements of hemoglobin concentration, oxygen saturation, and blood flow speed.

38. Wang LV, Hu S: **Photoacoustic tomography: in vivo imaging from organelles to organs**. *Science* Mar. 2012, **335**:1458–1462. https://doi.org/10.1126/science.1216210.

39. Bou Jawde S, Takahashi A, Bates JHT, Suki B: **An analytical model for estimating alveolar wall elastic moduli from lung tissue uniaxial stress-strain curves**. *Front Physiol* 2020, **11**. Accessed: May 31, 2022. [Online]. Available: https://www.frontiersin.org/article/10.3389/fphys.2020.00121.

40. Hsia CCW, Hyde DM, Weibel ER: **Lung structure and the intrinsic challenges of gas exchange**. In *Comprehensive physiology*. John Wiley & Sons; 2016:827–895. https://doi.org/10.1002/cphy.c150028.

41. ** Chen J, *et al.*: **Non-destructive vacuum-assisted measurement of lung elastic modulus**. *Acta Biomater* Sep. 2021, **131**: 370–380. https://doi.org/10.1016/j.actbio.2021.06.037.
This paper describes an imaging-assisted non-destructive tissue stiffness measurement method. By correlating the length of lung tissue elongated and the magnitude of vacuum pressure applied to induce the tissue deformation, elastic moduli of soft lung tissue can be accurately determined in real time.

42. Bohadana A, Izbicki G, Kraman SS: **Fundamentals of lung auscultation**. *N Engl J Med* Feb. 2014, **370**:744–751. https://doi.org/10.1056/NEJMra1302901.

43. Heil M, Hazel AL: **Fluid-structure interaction in internal physiological flows**. *Annu Rev Fluid Mech* 2011, **43**:141–162. https://doi.org/10.1146/annurev-fluid-122109-160703.

44. Hozain AE, *et al.*: **Multiday maintenance of extracorporeal lungs using cross-circulation with conscious swine**. *J Thorac Cardiovasc Surg* Apr. 2020, **159**:1640–1653. https://doi.org/10.1016/j.jtcvs.2019.09.121. e18.

45. Sage E, *et al.*: **Real-time computed tomography highlights pulmonary parenchymal evolution during ex vivo lung reconditioning**. *Ann Thorac Surg* Jun. 2017, **103**:e535–e537. https://doi.org/10.1016/j.athoracsur.2016.12.029.

46. Tane S, Noda K, Hayanga AJ, D'Cunha J, Luketich JD, Shigemura N: **Microvasculature analysis using micro CTA techniques for lungs after different preservation process**. *J Heart Lung Transplant* Apr. 2017, **36**:S90. https://doi.org/10.1016/j.healun.2017.01.227.

47. Renne J, *et al.*: **Functional pulmonary magnetic resonance imaging for detection of ischemic injury in a porcine ex-vivo lung perfusion system prior to transplantation**. *Acad Radiol* Feb. 2019, **26**:170–178. https://doi.org/10.1016/j.acra.2018.05.006.

48. R. Kosaka *et al.*, "Lung thermography during the initial reperfusion period to assess pulmonary function in cellular ex vivo lung perfusion," Artif Organs, vol. n/a, no. n/a, doi: 10.1111/aor.14219.

49. ** Ayyat KS, *et al.*: **A CLUE for better assessment of donor lungs: novel technique in clinical ex vivo lung perfusion**. *J Heart Lung Transplant* Nov. 2020, **39**:1220–1227. https://doi.org/10.1016/j.healun.2020.07.013.
Ayyat et al. report an ultrasound-based methodology for monitoring extravascular lung water during EVLP. In a clinical study of lung transplantation, CLUE (direCt Lung Ultrasound Evaluation) scores were significantly different in suitable versus non-suitable donor lungs and correlated with transplant outcomes.

50. Dorrello NV, *et al.*: **Functional vascularized lung grafts for lung bioengineering**. *Sci Adv* Aug. 2017, **3**, e1700521. https://doi.org/10.1126/sciadv.1700521.

51. * Nykänen AI, *et al.*: **Near-infrared fluorescence imaging during ex vivo lung perfusion: noninvasive real-time evaluation of regional lung perfusion and edema**. *J Thorac Cardiovasc Surg* Mar. 2022. https://doi.org/10.1016/j.jtcvs.2022.02.048.
Nykänen et al. utilized near-infrared fluorescence (NIRF) imaging to visualize indocyanine green delivered intravenously. NIRF imaging allowed assessment of pulmonary vascular perfusion and edema in both swine and human donor lungs supported on EVLP.

52. A. Marshall, T. R. Choudhary, N. Krstajic, M. G. Tanner, H. Parker, and M. Bradley, "Optical assessment of pulmonary vascular leak using a model of ex vivo lung perfusion," p. 2.

53. Naumova AV, Modo M, Moore A, Murry CE, Frank JA: **Clinical imaging in regenerative medicine**. *Nat Biotechnol* Aug. 2014, **32**. https://doi.org/10.1038/nbt.2993. Art. no. 8.

54. Park I, *et al.*: **Neutrophils disturb pulmonary microcirculation in sepsis-induced acute lung injury**. *Eur Respir J* Mar. 2019, **53**. https://doi.org/10.1183/13993003.00786-2018.

55. Yipp BG, *et al.*: **The lung is a host defense niche for immediate neutrophil-mediated vascular protection**. *Sci. Immunol.* Apr. 2017, **2**, eaam8929. https://doi.org/10.1126/sciimmunol.aam8929.

56. Masterson CH, *et al.*: **Intra-vital imaging of mesenchymal stromal cell kinetics in the pulmonary vasculature during infection**. *Sci Rep* Mar. 2021, **11**:5265. https://doi.org/10.1038/s41598-021-83894-7.